Chem. Senses 34: 667–678, 2009
doi:10.1093/chemse/bjp046
Advance Access publication July 30, 2009

Seasonal Increase in Olfactory Receptor Neurons of the Japanese Toad, *Bufo japonicus*, is Paralleled by an Increase in Olfactory Sensitivity to Isoamyl Acetate

Hideo Nakazawa[1], Masumi Ichikawa[2] and Takatoshi Nagai[1]

[1]Department of Biology, School of Medicine, Keio University, 4-1-1 Hiyoshi, Yokohama 223-8521, Japan and [2]Laboratory of Anatomy and Cell Biology, Department of Neuroscience Basic Technology, Tokyo Metropolitan Institute for Neuroscience, Tokyo 183-8526, Japan

Correspondence to be sent to: Hideo Nakazawa, Department of Biology, School of Medicine, Keio University, 4-1-1 Hiyoshi, Yokohama 223-8521, Japan. e-mail: hideonak@hc.cc.keio.ac.jp

Abstract

Japanese toads (*Bufo japonicus*) migrate to and from breeding sites in the early spring, possibly guided by olfactory cues. We previously showed that the electrical activity of olfactory receptor neurons (ORNs) in the toads was enhanced in the breeding period. We undertook morphological and physiological studies of the olfactory epithelium to determine whether any cellular substrate of the epithelium underlies the enhanced electrical activity of ORNs. The ORNs of the toads were labeled by antiserum to olfactory marker protein (OMP), and the morphology of the labeled cells and their distribution in the epithelium were examined throughout the year. The OMP-positive cells, distributed mainly in the basal and intermediate layers of the epithelium, were most numerous in the early breeding period. Cell proliferation in the epithelium detected by 5-bromo-2′-deoxyuridine labeling was most elevated in this period. The electrical activity of ORNs was examined by recording the electroolfactogram (EOG) in the toads throughout the year. Statistical analysis showed a positive correlation between the density of OMP-positive cells in the epithelium and the amplitude of the EOG responses. A greater number of ORNs in the breeding period possibly aids the toads in migrating to their breeding sites.

Key words: amphibian, breeding, electroolfactogram, olfactory epithelium, ORN

Introduction

Most amphibians forage for food in their home ranges during most of the year. In the breeding season, however, they move to breeding sites even a kilometer or more overland and return to their home ranges (Stille 1952; Pilliod et al. 2002). The breeding sites are normally their birthplace, specific to the species of amphibians or a group of animals (Dingle 1996). Such fidelity to the breeding site has been reported for a number of amphibian species (Twitty 1959; Whitford and Vinegar 1966; Dole 1968; Gill 1978; Berven and Grudzien 1990). As to how amphibians can achieve lengthy migrations to and from the breeding site, various sensory cues are proposed to play a role. These include olfactory (Grubb 1973; Sinsch 1987), visual (Sinsch 1992), auditory (Schmidt 1984), and magnetosensory (Phillips 1987; Sinsch 1987) cues.

The anuran amphibian, Japanese toads (*Bufo japonicus*), also exhibits fidelity to their breeding sites (Kusano et al. 1995, 1999). They migrate in early spring to certain ponds for mating and spawning. Ishii et al. (1995) observed that the toads returned to their home range along the same migration route and that anosmic operation on the nasal mucosa made the toads disoriented on the route while leaving their locomotion activity intact. They speculated that the toads memorize the route or area of their migration by using the olfactory sense.

In response to odor stimulation, a slow potential change is recorded from the surface of the olfactory epithelium. Ottoson (1958) termed the slow potential the electroolfactogram (EOG) in his recording of the olfactory response in common frogs (*Rana temporaria*). The EOGs are thought to originate from the electrical activities induced in a large number of olfactory receptor neurons (ORNs; Ottoson 1956; Takagi and Yajima 1964). We previously studied the EOGs in Japanese toads collected throughout the year and found that the EOGs were enhanced in a period that includes the breeding season (Nakazawa et al. 2000). We also observed that oscillatory potentials superimposed on the EOG became evident particularly in the breeding season of the toads. The

oscillatory potentials in the olfactory epithelium were first reported in mammals by Adrian (1955, 1956) and then in other vertebrates (fish [Sutterlin AM and Sutterlin N 1971; Suzuki et al. 2004], amphibians [Ottoson 1956; Takagi and Shibuya 1960], reptiles [Tucker 1975; Lam et al. 2000], and birds [Shibuya and Tucker 1967]). A study on the salamander olfactory system suggested that spiking activity of the ORNs is a source of oscillations in the olfactory epithelium (Dorries and Kauer 2000). In the channel catfish olfactory epithelium, the oscillations were hypothesized to function to modulate neural activities in the higher center of olfactory pathways, the olfactory bulb (Nikonov et al. 2002). In other neural systems such as higher visual neurons, a functional role of oscillations has been suggested by various experimental approaches (Gray and Singer 1989; Ghose and Freeman 1992), but not explicitly demonstrated except by a neurophysiological study combined with behavioral discrimination of odorants in honeybees (Stopfer et al. 1997). In the present study, we examined oscillations in the olfactory epithelium of Japanese toads more quantitatively than our previous study. In parallel with electrophysiological experiments on the toads collected in the field throughout the year, we also examined the morphology of the olfactory epithelium in those toads. Studies in the red-backed salamander showed that morphological changes in the olfactory and the vomeronasal organs are associated with the breeding season of the animal (Dawley and Crowder 1995; Dawley et al. 2000). Similar changes may occur in the toads that show olfactory-mediated behavior in the breeding season. The present study obtained morphological and physiological evidence to support the olfactory hypothesis of migratory behavior in the Japanese toads.

Materials and methods

Animals

Adult males of the Japanese toad (*Bufo japonicus formosus* Boulenger, 1883) were collected at a park in Tokyo with the permission of the administration office of Tokyo Metropolitan Park Association and immediately used for experiments. The toad's life cycle consists of following 3 periods. The toads actively prey on small animals through a period from April to November, termed the foraging period, in the study area. From December to January, termed the torpid period, they burrow into the ground and become torpid. From February to March, termed the breeding period, they awake on humid and relatively warm nights from the winter torpor and start to migrate to their breeding pond. Soon after mating and spawning in the pond, they leave the pond and migrate back to their home range.

For the morphological experiment, we examined toads collected in the torpid period (December and January, n = 3, respectively), the breeding period (February, n = 6), and the foraging period (April, June, August, and October, n = 3, respectively). In the breeding period, in particular, we collected toads on the ground near the breeding pond in 2 phases: those when the toads were migrating to the breeding pond and migrating back to their home range (phase I and phase II, n = 3, respectively). We observed the animal's undisturbed movements on the ground to judge their direction of migration. For the electrophysiological experiment, we examined toads collected in December (n = 5), February (phase I, n = 9; phase II, n = 6), and October (n = 5). We chose animals of similar body size to minimize the variation in the olfactory epithelial volume. The average body size was 102.1 ± 0.9 mm (n = 24; mean ± standard error of the mean [SEM]) in the toads for the morphological experiment and 100.8 ± 0.9 mm (n = 25) for the electrophysiological experiment. In addition to these animals, we collected a group of toads in the torpid period for the experiment to probe the position of electrodes. All experiments were conducted according to the guideline of the Laboratory Animal Care and Use Committee of Keio University School of Medicine.

Tissue preparation

Animals were anesthetized by immersion into 0.5% tricaine methanesulfonate (TCI, Tokyo Kasei Kogyo Co., Ltd.) and perfused intracardially with ice-cold physiological saline followed by 4% paraformaldehyde (PFA) in 0.1 M phosphate buffer solution (pH 7.4) for fixation. Snouts were removed, postfixed in phosphate-buffered PFA (4%) for 1 h, and rinsed in phosphate-buffered 30% sucrose solution overnight at 4 °C. In Japanese toads, the olfactory epithelium covers a wide area of the olfactory cavity, the ventral wall of which protrudes to form thick eminentia olfactoria (Figure 1). The present study was focused on the olfactory epithelium that covers the center of the eminentia olfactoria because this flat area is easily accessible to an electrode for EOG recording. The eminentia olfactoria was excised from the snout, embedded in Tissue-Tek OCT compound (Sakura Finetek Japan Co., Ltd.) for cryostat sectioning, and kept in a deep freezer (–80 °C). In the center of the eminentia olfactoria (Figure 1A), coronal sections were cut at 10-μm thick with a cryostat (Microm HM500, Zeiss) and subjected to immunolabelings.

Labeling by antiserum to olfactory marker protein

ORNs were labeled by antiserum to olfactory marker protein (OMP): a marker for mature ORNs (Margolis 1972, 1988; Farbman and Margolis 1980). The antiserum to OMP was obtained by immunizing rabbits with histidine-tagged rat OMP that was produced in *Escherichia coli* expression system and purified by affinity chromatography (Takigami et al. 2004). The sections were incubated in a blocking solution consisting of 10% Block Ace (Dainippon pharmaceutical Co., Ltd.) and 0.1% Triton X-100 in 0.1 M phosphate-buffered saline (PBS) for 1 h, and then

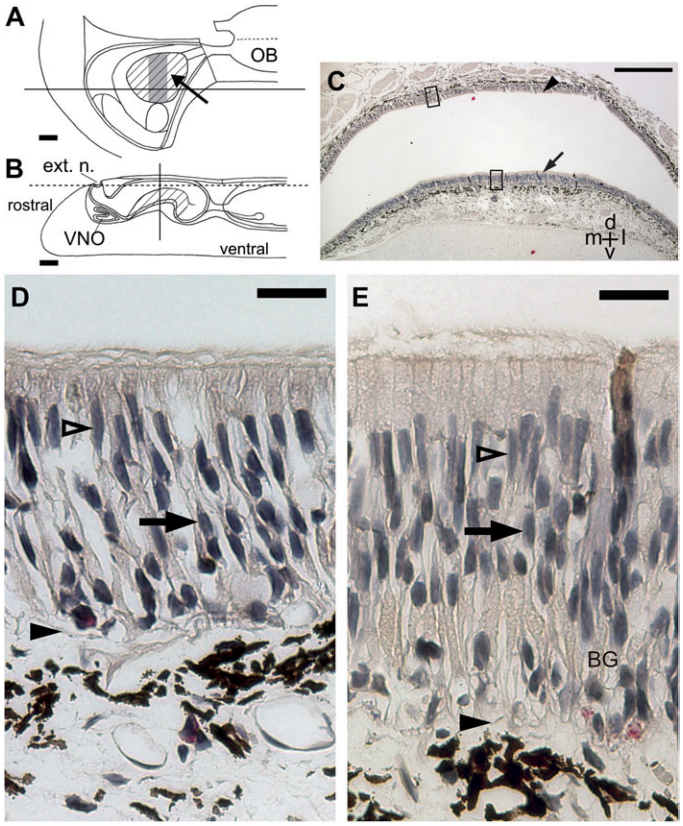

Figure 1 The olfactory cavity of *Bufo japonicus*. **(A)** Dorsal view. The dorsal wall of the olfactory cavity has been removed to show the eminentia olfactoria (arrowed hatched area). The middle of the eminentia olfactoria (shaded area) was examined in histological study. Horizontal line shows a sagital plane where the olfactory cavity was cut for lateral view. **(B)** Lateral view. Dotted line shows a horizontal plane where the dorsal wall was removed to create the dorsal view. **(C)** Coronal section of the left olfactory cavity of the toad collected in August. A paraffin-embedded tissue was sectioned through a vertical line shown in **(B)** at 4-μm thickness and stained with hematoxylin and eosin. Both dorsal wall and eminentia olfactoria are lined with the olfactory epithelium shown by arrowhead and arrow, respectively. **(D)** High-power view of the epithelium within the frame placed on the dorsal wall in **(C)**. **(E)** High-power view of the epithelium within the frame placed on the eminentia olfactoria in **(C)**. **(D** and **E)** Supporting cells with elongated nucleus (open arrowhead) and ORNs (arrow) are seen in the olfactory epithelium. The olfactory epithelium is thinner in the dorsal wall than in the eminentia olfactoria, as shown by upper location of the basement membrane in the dorsal wall (arrowhead). BG, Bowman's gland; ext. n., external naris; OB, olfactory bulb; VNO, vomeronasal organ. Scale bar = 1 mm in **(A** and **B)**, 500 μm in **(C)**, and 20 μm in **(D** and **E)**.

incubated with rabbit anti-OMP antiserum (1:150) for 20 h at 4 °C. Following 3 washings in PBS for 5 min each, the sections were incubated with Alexa Fluor 488 conjugated goat anti-rabbit secondary antibody (1:200, Molecular Probes, Inc.) for 1 h at 25 °C. After 3 washings in PBS for 5 min each, the sections were mounted in Vectashield mounting medium (Vector Laboratories, Inc.). Only background labeling was seen in control experiments, in which the primary antiserum or the secondary antibody was omitted (not shown).

BrdU labeling and detection

Cell proliferation was measured by 5-bromo-2′-deoxyuridine (BrdU) incorporation method. Animals were given a single injection of BrdU (Sigma) intraperitoneally at a dose of 5 mg/100 g body weight (5 mg/mL dissolved in saline) and sacrificed 1 h after the injection of BrdU. The coronal sections were rinsed with PBS, treated with 2 N HCl at 37 °C for 30 min, and rinsed with 0.1 M borate buffer (pH 8.5) 3 times for 5 min each. These sections were rinsed with PBS, incubated in a blocking solution for 1 h, and then incubated overnight at 4 °C with mouse anti-BrdU monoclonal antibody (1:25, Molecular Probes). After 3 washings in PBS for 5 min each, the sections were incubated for 2 h at 25 °C with Alexa Fluor 488 conjugated goat anti-mouse IgG_1 (1:200, Molecular Probes), as a secondary antibody. Only background labeling was seen in control experiments, in which the primary or the secondary antibody was omitted (not shown).

Counting of OMP-positive cells and BrdU-positive cells with fluorescence microscopy

Immunolabeled sections were examined with a confocal laser scanning microscope (Fluoview FV300, Olympus) equipped with differential interference contrast (DIC). To quantify the results, we selected the coronal sections each separated at 200 μm in the center of the eminentia olfactoria ($n = 3$, for OMP labeling; $n = 4$, for BrdU detection). In the OMP-positive cells, a short diameter of the cell body and the nuclear position were measured by ImageJ software (JAVA version of NIH Image). In BrdU-positive cells, the nuclear position was similarly measured. These measurements were performed in evenly divided 3 layers of the olfactory epithelium: the basal, intermediate, and apical layers because there was no significant difference in the thickness of the olfactory epithelium throughout the year (133.7 ± 4.1 μm, $n = 24$, $P = 0.118$ by 1-way analysis of variance [ANOVA]). The cell count was divided by the length of the olfactory epithelium to yield a density of the cells per unit length. There was no significant difference in the size of OMP-positive cells among either the layers of the olfactory epithelium (basal layer, 6.12 ± 0.04 μm, $n = 123$; intermediate layer, 6.12 ± 0.03 μm, $n = 161$; apical layer, 6.10 ± 0.03 μm, $n = 30$; mean ± SEM) or 3 periods of toad's life cycle. Therefore, the cell count was not corrected by Abercrombie's equation (Abercrombie 1946).

Application of odorants

The olfactory epithelium was continuously exposed to the humidified air applied through a guide nozzle (internal diameter 5.5 mm) placed at a distance of 1 cm from the eminentia olfactoria. The air was applied to the epithelium at a constant flow rate of 6.5 mL/s driven by the pressure from a diaphragm pump. Odor stimulus was given by switching the air to odorized air for 4 s using a custom-made olfactory stimulator

controlled by solenoid valves. The odorized air was prepared by passing filtrated air to a glass bottle containing isoamyl acetate solution at concentrations of 0.005, 0.05, 0.5, 5, and 50 mM. The 50 mM was a nominal solution, which yielded saturated vapor of isoamyl acetate. Isoamyl acetate was chosen as a species of odorant because it gives a large, robust response and is often used as a standard stimulus in EOG recordings. Isoamyl acetate is an odor that can be emitted from vegetation, fungi, and bacteria in the environment (Kiviranta et al. 1998; Schomburg et al. 2006), thus possibly a biologically relevant odor for the toad. The odorized air of each concentration was given in a random sequence at an interval of 2 min. The series of odor stimuli consisting of 5 concentrations were repeated 3 times. At the start of odor stimulation, a blank stimulus was given to estimate a possible mechanical response to the switching of airflow. Induced mechanical response was subtracted from the responses to the odorized air.

Recording of EOG responses

Animals were anesthetized by immersion in 0.5% tricaine methanesulfonate and pithed for immobilization. The dorsal wall of olfactory cavity was removed to place the Ag–AgCl recording electrode (0.2-mm diameter) at the center of the eminentia olfactoria for EOG recording (Figure 1). The reference electrode (Ag–AgCl plate, 5×5 mm^2) was placed on the surface of the cranium at a distance of 15 mm from the site where the recording electrode was placed. The EOGs were differentially amplified (AVB-21, Nihon Kohden) and stored on a PC with PowerLab 4/20 (ADInstruments Pty Ltd.) for further analysis.

Statistical analysis

Data are expressed as mean ± SEM (in the studies of the density of immunolabeled cells and the amplitude of EOG responses). Statistical comparisons of means were made by 1-way ANOVA followed by Tukey's honestly significant difference (HSD) test. Before conducting ANOVA, Bartlett's test was used to assess heterogeneity of variances among groups being compared. If the heterogeneity of variance was significant, Kruskal–Wallis test was used instead of ANOVA. Kruskal–Wallis test was followed by Bonferroni-corrected Mann–Whitney U test. The correlation between the amplitude of EOG responses and the density of OMP-positive cells was analyzed with the Pearson's correlation coefficient.

Results

OMP-positive cells in the olfactory epithelium

Anti-OMP antiserum labeled numerous cells with a spindle-shaped cell body and a narrow dendrite extending to the surface of the epithelium (Figure 2A,B). On the top of the epithelium, brightly fluorescent dendritic knobs were associated with ciliary bundles shown by DIC image (Figure 2C,D). These morphological features are reminiscent of the mature olfactory receptor cell. The spindle-shaped cells labeled by anti-OMP antiserum were usually seen in the intermediate layer (Figures 2A and 3D).

Structural organization of the olfactory epithelium in the toads collected throughout the year

In the torpid period, the OMP-positive cells with a round-shaped cell body were densely distributed in the basal and intermediate layers of the olfactory epithelium (Figure 3A). In the early breeding period (phase I), the cells with a spindle-shaped cell body appeared in the intermediate layer, whereas the cells with a round-shaped cell body remained dense in the basal layer (Figure 3B). In the late breeding period (phase II), the cells were dense in the intermediate layer, whereas they were sparsely distributed in the basal layer (Figure 3C). In the foraging period, the distribution of the cells with a spindle-shaped cell body centered in the intermediate layer (Figure 3D). Overall patterns of distribution of OMP-positive cells throughout the year show a transition from the basal to the intermediate layer.

Distribution of OMP-positive cells in the olfactory epithelium

The density of OMP-positive cells in the epithelium gradually increased in the torpid period, reached a peak in the early breeding period (phase I), and rapidly decreased in the late breeding period (phase II; Figure 4). After gradually decreasing at the end of the breeding period through the early foraging period, the density of the cells reached a minimum at the end of the foraging period (October). Seasonal fluctuation in the cell density was further examined in 3 layers of the olfactory epithelium (the basal, intermediate, and apical layers, see Figure 3). In the apical layer, OMP-positive cells were few in the torpid period and remained so in the breeding and foraging periods (Figure 4, black triangles; see also Figure 3). Therefore, the majority of the cells are of the basal and intermediate layers. The cell density in the basal layer peaked in phase I, decreased by about 25% of the total cells in phase II, and then gradually decreased in the foraging period (Figure 4, white squares). On the other hand, the cell density in the intermediate layer slightly increased in phase II (Figure 4, black squares; phase I vs. phase II, $P < 0.05$ by 1-tailed t-test) and the density in that phase was maintained, although with a slight reduction, throughout the foraging period. Therefore, the decrease in OMP-positive cells in the olfactory epithelium in phase II as well as in the periods that follow seemed to be caused by a reduction of the cells in the basal layer.

To study if the increase in the cells in the intermediate layer in phase II was caused by generation of the cells in that layer or migration of the cells from other layers, we measured cell proliferation by BrdU incorporation method (Figures 5 and 6). Generally, the cell proliferation was high in the basal layer

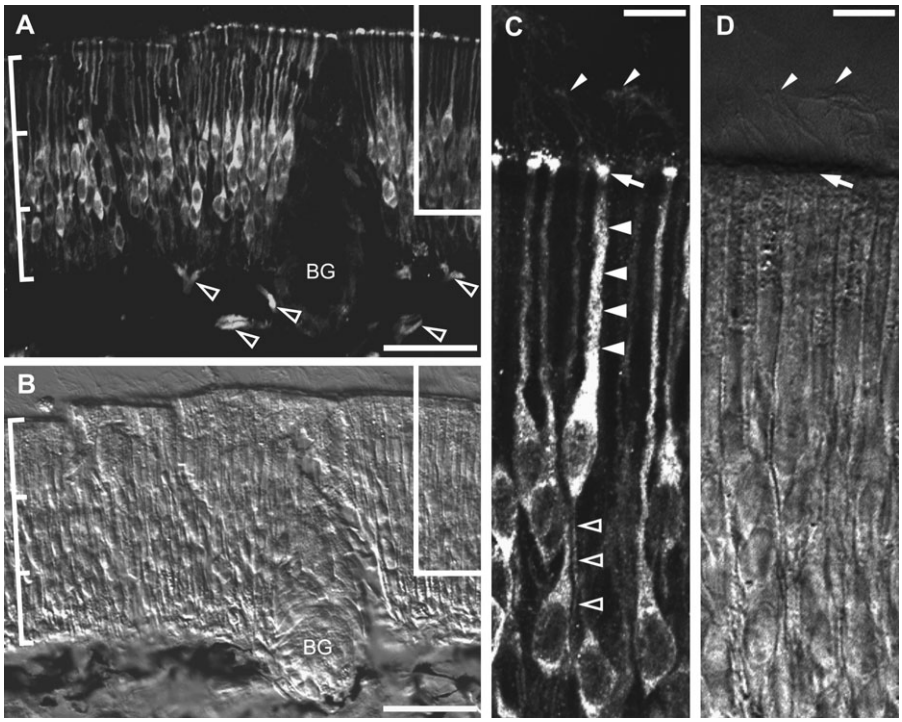

Figure 2 OMP-positive cells in the olfactory epithelium of the toad collected in August. **(A)** Fluorescent image of cross-sectioned tissue. The lamina propria contains OMP-positive nerve fibers (open arrowheads). **(B)** The corresponding DIC image. **(C)** Rectangular area indicated on the photomicrograph **(A)** was examined with a high-power objective (60×). Brightly fluorescent cells with a single process (arrowheads) extend to the apical surface of epithelium, where a knob-like protrusion (arrow) gives ciliary bundles (small arrowheads, see also Figure 2D). Axonal fibers (open arrowheads) extend into the basal layer. **(D)** The corresponding DIC image. BG, Bowman's gland. Scale bar = 50 μm in **(A** and **B)**, 10 μm in **(C** and **D)**. The vertical scale in **(A** and **B)** indicates equally divided 3 layers in the olfactory epithelium for analysis.

and very low in the intermediate and apical layers throughout the year (Figure 6). No significant increase in the proliferation in the intermediate layer occurred in phase II. On the other hand, the highest proliferation in the basal layer occurred in phase I, which is the phase just before the OMP-positive cells in the intermediate layer increased (see phase II in Figure 4). Therefore, the increase in the cells in the intermediate layer in phase II must be induced by migration of the cells from the basal layer. The proliferation in the basal layer was rapidly reduced in phase II and gradually resumed toward the late foraging period. Resumed cell proliferation probably alleviated the reduction of the cells in the basal layer (see Figure 4).

EOG responses in *B. japonicus*

First, we probed the position of recording electrode in the mucous layer that covers the olfactory epithelium because the magnitude of the EOG responses may vary depending on the distance between the tip of the electrode and the surface of the olfactory epithelium. The recording electrode was advanced to the center of the eminentia olfactoria using a micromanipulator (SM-15, Narishige Co., Ltd.). When the tip of the electrode made contact with the surface of the mucous layer under visual guide, the position of electrode was defined as 0 μm. The electrode was further advanced at 10-μm steps. At each step, the EOG was recorded to the odor stimulus of 0.5 mM isoamyl acetate (Figure 7A). The magnitude of the EOG responses did not vary very much between position 0 and 160 μm but started to decrease at positions deeper than 160 μm (Figure 7A,B). At deeper positions, the surface of the olfactory epithelium was slightly distorted around the tip of the electrode, showing that the electrode came in firm contact with the surface. We found that the magnitude of EOG responses was not statistically different at positions from 0 to 160 μm (n = 5, toads collected in the torpid period, $P > 0.05$ by Tukey's HSD test; Figure 7C). Therefore, in the following series of odor stimulations, we placed the recording electrode in the mucous layer so as not to make firm contact with the olfactory epithelium.

Odor stimulation to the olfactory epithelium induced a negative slow potential in a concentration-dependent manner (Figure 8). In most cases, stimuli at higher concentrations (5, 50 mM isoamyl acetate) induced oscillatory potentials superimposed on the late phase of the slow potentials. In phase I, also at a lower concentration (0.5 mM), very small oscillations were induced (Figure 8, the response at 0.5 mM). Therefore, we evaluated the EOG responses by 2 measures: the amplitude of a negative slow potential at peak and the amplitude of an oscillation at peak during

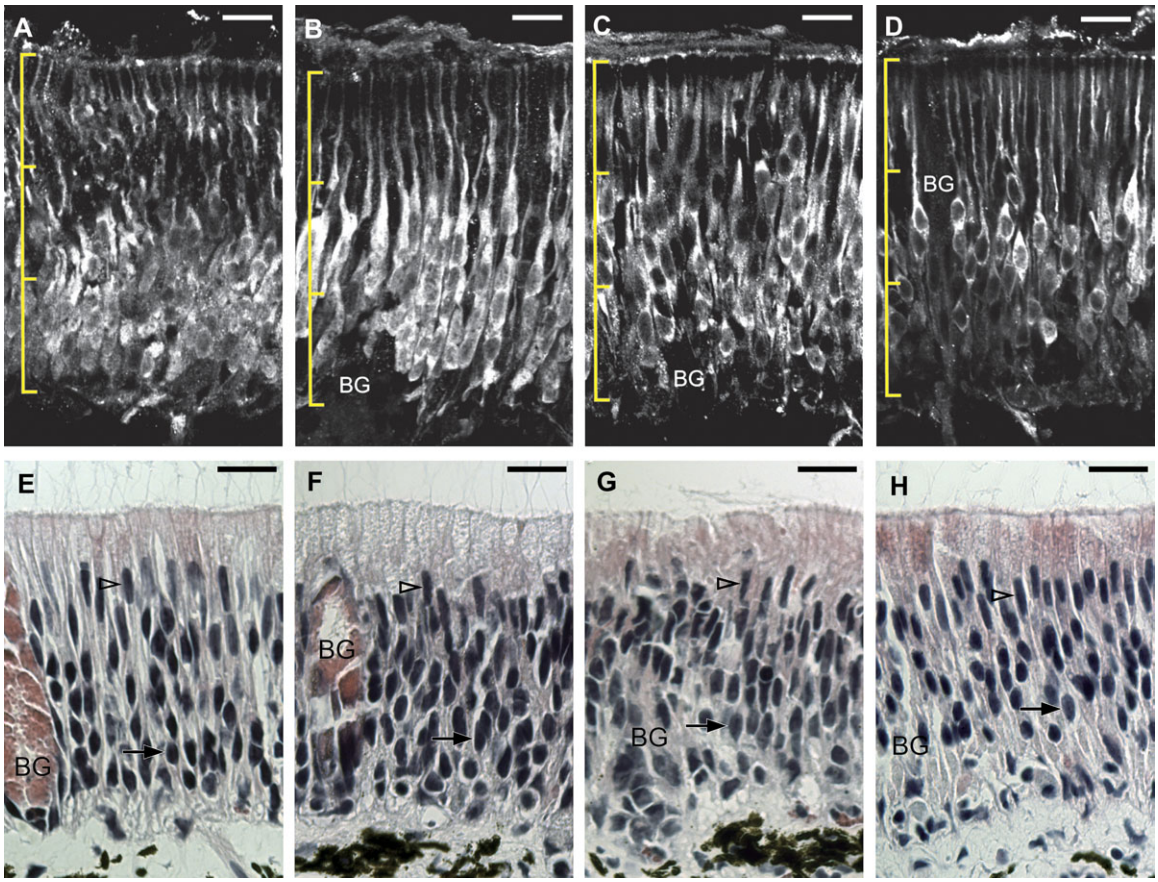

Figure 3 Distribution of OMP-positive cells in the olfactory epithelium. **(A)** Fluorescent image of cross-sectioned tissue obtained from the toad collected in the torpid period (December). **(B)** Fluorescent image from the toad collected in the early breeding period (phase I). **(C)** Fluorescent image from the toad collected in the late breeding period (phase II). **(D)** Fluorescent image from the toad collected in the foraging period (October). Note the layer of the epithelium where cell bodies of OMP-positive cells are distributed. **(E–H)** Photomicrographs of hematoxylin and eosin-stained sections of the olfactory epithelium (paraffin-embedded tissue) in the periods corresponding to **(A)** to **(D)**, respectively. Supporting cells with elongated nucleus (open arrowhead) and ORNs (arrow) are seen in the olfactory epithelium. The nuclei of the supporting cells were distributed in the apical layer of the epithelium. Relative location of those cells in the epithelium of the eminentia olfactoria did not change throughout the year. BG, Bowman's gland. Scale bar = 20 μm. These specimens were examined with a 40× objective.

olfactory stimulation (Figure 8). Using these measures, we studied the intensity-response curve for isoamyl acetate in the toads collected in the torpid period, the breeding period (phase I and phase II), and the foraging period (Figure 9A,B). The slow potentials were induced at concentrations of 0.05 mM and above in those toads. Stimuli at 50 mM induced the responses at plateau in most toads except those in phase II of the breeding period. Generally, the slow potentials recorded in the torpid and breeding periods were larger than those in the foraging period (Figure 9A). The oscillations in the EOGs were induced at 0.5 mM and above, and this threshold concentration was 10-fold higher than that for the slow potentials (Figure 9B). The oscillations were always observed in the torpid and breeding periods. In the foraging period, however, almost no oscillations were induced at all concentrations (Figure 9B).

To study a possible seasonal change in the EOG responses, we focused on the responses induced at 50 mM because those were near-maximum responses (Figure 9). When evaluated by either slow potentials or oscillations, the EOG responses in the breeding period (phase I) were significantly larger than those in the foraging period (for slow potentials, $P < 0.05$ by Tukey's HSD test; for oscillations, $P < 0.05$ by Bonferroni-corrected Mann–Whitney U test; Figure 10A). The results showed that the EOG responses in the breeding period (phase I) were the largest of the 3 periods. The total density of OMP-positive cells in this period was the highest of the year (Figure 4). Therefore, to study a possible correlation between the amplitude of EOG responses and the density of OMP-positive cells, a part of the data shown in Figure 4 was selected and plotted against the 3 periods of toad's life cycle (Figure 10B). Being evaluated by either slow potentials or oscillations, the amplitude of EOG responses was positively correlated with the total density of OMP-positive cells ($r = 0.765$ for slow potentials; $r = 0.887$ for oscillations; Figure 11 and Table 1). A correlation analysis was further

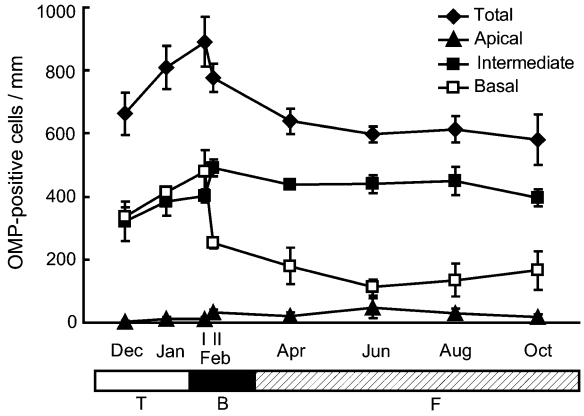

Figure 4 Regional distribution of OMP-positive cells in the olfactory epithelium throughout the year. OMP-positive cells were counted in 3 layers of the epithelium: apical (black triangles), intermediate (black squares), and basal (white squares). The counts in 3 layers were summed (black diamonds). Ordinate: The density of OMP-positive cells. Abscissa: Months of collection. Data are indicated as mean ± SEM for each point (n = 3). The life history of *Bufo japonicus* is indicated under the abscissa: T, torpid period; B, breeding period; F, foraging period.

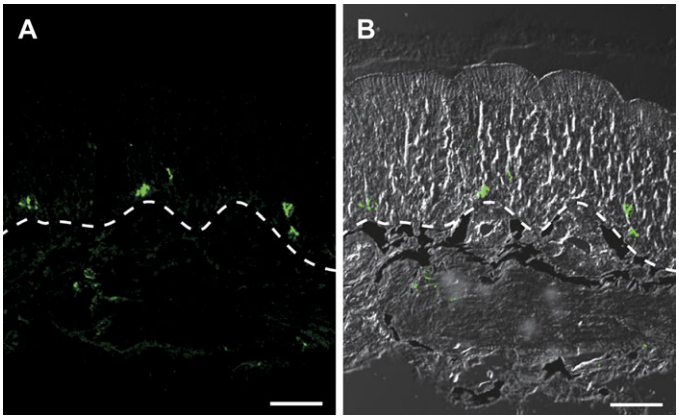

Figure 5 BrdU immunodetection of mitotically active cells in the olfactory epithelium. **(A)** Fluorescent image of BrdU-positive cells in the olfactory epithelium in the early breeding period (phase I). A dashed line indicates the position of the basement membrane. **(B)** Fluorescent image in **(A)** is overlaid on DIC image. Scale bar = 50 μm.

performed in the different layers of the olfactory epithelium (Table 1). The amplitude of oscillations was significantly correlated with the density of OMP-positive cells in the basal layer (r = 0.948, P = 0.026 < 0.05, n = 4).

Discussion

Neurons labeled by anti-OMP antiserum in the olfactory epithelium of the toads

The antiserum used in the present study was obtained by immunizing rabbits with the rat OMP. This antiserum successfully labeled the ORNs and the vomeronasal neurons in mammalian species (Takigami et al. 2004; Moriya-Ito et al.

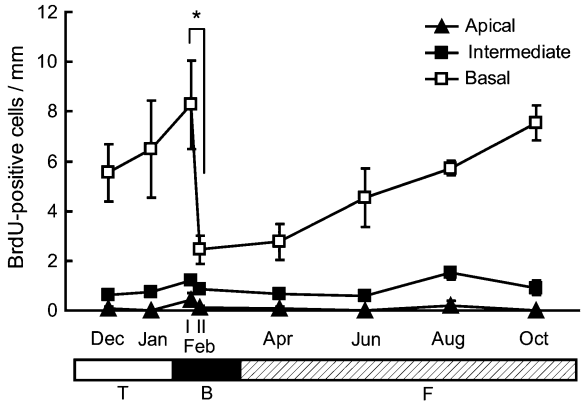

Figure 6 Regional distribution of BrdU-positive cells in the olfactory epithelium throughout the year. The cells were counted in each of 3 layers of the epithelium: apical (black triangles), intermediate (black squares), and basal (white squares) layer. A large population of the cells was distributed in the basal layer, where a drastic change in cell proliferation occurred in the breeding period. In the intermediate and the apical layers, cell proliferation was low throughout the year. Ordinate: The density of BrdU-positive cells. Abscissa: Months of collection. Data are indicated as mean ± SEM for each point (n = 3). Asterisk indicates a statistically significant difference (P < 0.05 by Tukey's HSD test). The life history of *Bufo japonicus* is indicated under the abscissa: T, torpid period; B, breeding period; F, foraging period.

2005). Similar antiserum raised against the rat OMP had proven to be useful to identify mature ORNs in amphibian species (Keller and Margolis 1975; Krishna et al. 1992). Phylogenetic conservation in the sequence of OMP has been suggested by immunohistochemical studies of the olfactory system in other nonmammalians: teleost (Riddle and Oakley 1992) and cartilaginous fish (Ferrando et al. 2007). Therefore, the present study used anti-rat OMP antiserum to discriminate mature ORNs from precursor cells and supporting cells in the olfactory epithelium of the toads. The anti-rat OMP antiserum clearly labeled the cilia, dendrites, cell bodies, and axons of the ORNs in the olfactory epithelium of the toads.

The OMP-positive cells in the basal layer of olfactory epithelium were almost as many as those in the intermediate layer in the torpid and the early breeding periods of the toads (Figure 4). This is in contrast with the development of OMP-positive cells in the mammalian olfactory epithelium. The ORNs in the basal layer are immature and thus OMP negative (Verhaagen et al. 1989), and they migrate to become OMP positive in the intermediate layer (Monti-Graziadei et al. 1977; Verhaagen et al. 1989). In the toads, the maturation of ORNs seems to precede the migration of those cells to the intermediate layer. It is noteworthy that when OMP-positive cells are abundant in the basal layer, the toads showed large EOG responses.

Cell proliferation in the olfactory epithelium

In adult vertebrate brains, cell proliferation of the neuron, namely neurogenesis, occurs in the brain regions such as

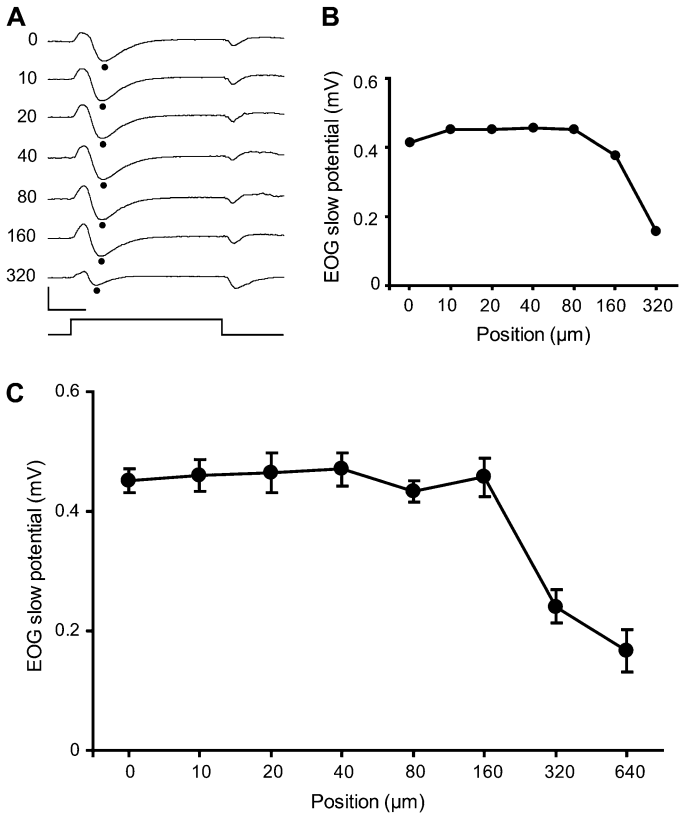

Figure 7 EOG responses recorded at different depths in the mucous layer on the olfactory epithelium of *Bufo japonicus*. **(A)** Sample records of EOG responses induced by 0.5 mM isoamyl acetate for 4 s. Position of the electrode in the mucous layer is shown in micrometer on the left of traces. The peak of a negative slow potential is marked with a black circle. The bottom trace shows the onset of stimulation. Bar = 1 s (horizontal) and 0.5 mV (vertical). **(B)** The magnitude of the EOG responses is measured at the peak of a negative slow potential in the sample records and plotted against positions of the electrode. **(C)** The magnitude of the EOG responses in 5 animals is summarized.

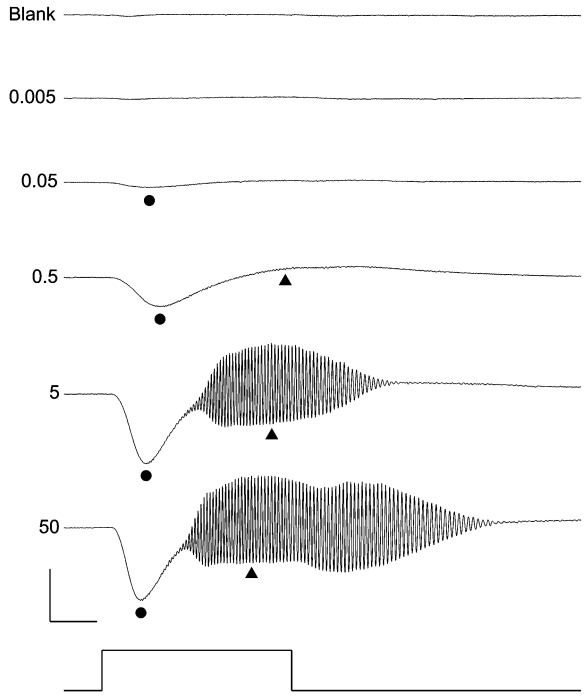

Figure 8 EOG responses in the olfactory epithelium of *Bufo japonicus* collected in the breeding period (phase I). Isoamyl acetate at a series of concentrations was applied to the olfactory epithelium for 4 s. Each concentration is shown in millimolar on the left of traces. Note that oscillations were induced at higher concentrations. The frequency of oscillations was about 14–16 Hz in the animals collected in phase I. The peaks of a negative slow potential and an oscillation are marked with a black circle and a black triangle, respectively. The bottom trace shows the onset of stimulation. Bar = 1 s (horizontal) and 1 mV (vertical).

the olfactory bulb and the hippocampus (Lledo et al. 2006). In the olfactory system not only the brain neurons but also the peripheral neurons undergo neurogenesis. The ORNs in the olfactory epithelium are continuously replaced throughout the life of the animal (Moulton 1974; Graziadei and Monti-Graziadei 1978; Farbman 1990) possibly to compensate for the cells lost by mechanical or chemical stress imposed by the environment. The present study showed that the mitotic activities in the olfactory epithelium of the toads were not maintained constant but were seasonal. Cell proliferation gradually increased in the foraging period and the torpid period and peaked in the early breeding period. A similar surge of the cell proliferation was reported in the olfactory epithelia of red-backed salamanders, which use the olfactory and vomeronasal organs to detect chemical cues for initiating behaviors in the home range (Graves 1994; Dawley 1998). Using the BrdU incorporation technique, Dawley et al. (2000) showed the rate of cell proliferation in the olfactory epithelium became greatest in the last month of the courtship season for the animal. They hypothesized that the seasonal upregulation of cell proliferation in the olfactory epithelium is induced in anticipation of seasonal events such as territorial behavior and mating.

The Japanese toads are able to orient to their breeding pond with high fidelity. Behavioral observation on these toads suggested that they rely on olfactory signals in the environment to orient to their breeding site (Ishii et al. 1995). To detect guiding signals from a wide array of odor molecules in the environment, the olfactory organ must acquire a higher sensitivity to the signals. Larger number of ORNs in the olfactory epithelium would be favorable to such detection. Increasing ORNs in the torpid period may ensure the olfactory sensitivity for the toads during the orientation. Season-dependent olfactory cellular proliferation also occurs in salmon, which use olfactory memory of their natal stream as a guide for homing migrations (Lema and Nevitt 2004). The cell proliferation during a particular time of the year is possibly related to imprinting natal stream odors. Therefore, the function of neurogenesis in the olfactory epithelium would be not simply to compensate for the lost cells but to facilitate sensory transduction in the receptor cells. Such a notion was further supported by the present physiological experiments as discussed below.

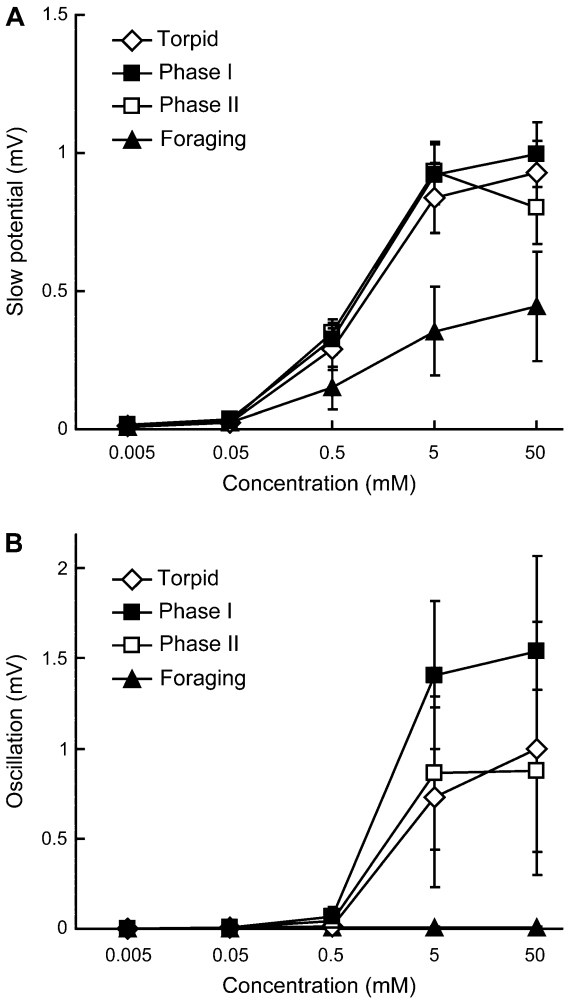

Figure 9 Intensity-response curves for isoamyl acetate in *Bufo japonicus* collected in the torpid period (white diamonds), the breeding period phase I (black squares) and phase II (white squares), and the foraging period (black triangles). **(A)** The response curves when the EOGs were evaluated by negative slow potentials. **(B)** The response curves when the EOGs were evaluated by oscillations. Ordinate: The amplitude of EOGs. Abscissa: Concentration of the olfactory stimuli. Data are expressed as mean ± SEM for each point (n = 5–9).

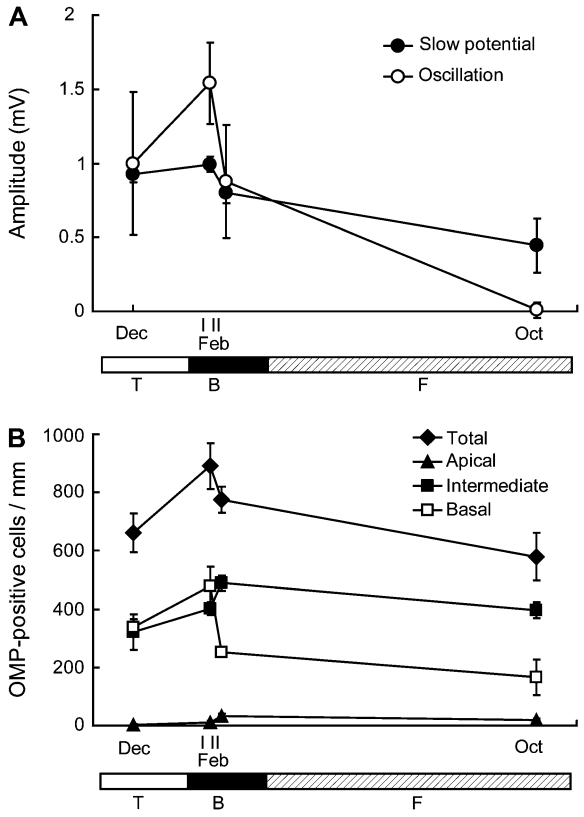

Figure 10 Seasonal change in the EOG responses possibly correlated with distribution of the OMP-positive cells in the olfactory epithelium. **(A)** The EOG responses at 50 mM were evaluated by negative slow potentials (black circles) and oscillations (white circles). Note that seasonal change of the EOG responses is the most conspicuous when the EOGs are evaluated by oscillations. Note also that the enhanced EOGs are accompanied by large increase in OMP-positive cells in phase I. Ordinate: The amplitude of EOGs. Abscissa: Months of collection. Data are indicated as mean ± SEM for each point (n = 5–9). **(B)** A part of the data shown in Figure 5 is selected to show a possible correlation between the amplitude of EOGs and the density of OMP-positive cells. Ordinate: The density of OMP-positive cells. Abscissa: Months of collection. Data are indicated as mean ± SEM for each point (n = 3). The life history of *Bufo japonicus* is indicated under the abscissa: T, torpid period; B, breeding period; F, foraging period.

EOG responses in relation to the electrodes

In the present study, the EOG responses in the toads collected at different times of the year were compared without subjecting those to analytical procedures such as normalization by a standard response. Criticisms on our method may be argued as follows. One criticism may be that the magnitude of the EOG responses varies with the distance between the tip of the recording electrode and the surface of the olfactory epithelium. However, as shown in Figure 7, the magnitude of the EOG responses did not vary significantly, possibly owing to relatively high conductivity of the mucus. Other criticism may be that the distance between the recording site and the reference electrode affects the magnitude of the EOG responses. This distance was kept constant in the present study (see Materials and methods). However, we performed a separate experiment to see if the EOG responses vary depending on the distance. When the reference electrode was shifted to either 5 mm rostral or caudal on the cranium, the magnitude of the EOG responses varied to some extent but only by less than 1.5% (n = 10). Therefore, a seasonal change in the EOGs is not likely to be derived from physical factors around either recording or reference electrode but most likely from a biological change in the toad ORNs such as their population and activity.

Enhancement of EOG responses in the breeding period

When the profile of EOG responses recorded throughout the year was studied in parallel with that of OMP-positive cells in the olfactory epithelium, overall profiles suggest that the

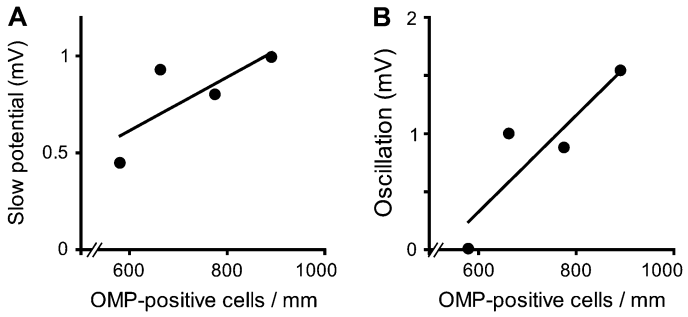

Figure 11 Correlation between the total density of OMP-positive cells in the olfactory epithelium and the amplitude of negative slow potentials **(A)** or the amplitude of oscillations **(B)**. Ordinate: The amplitude of EOGs. Abscissa: The total density of OMP-positive cells. The mean values in each period of toad's life cycle shown in Figure 10A,B (total) were selected for a correlation analysis. Linear regression is shown by a solid line.

Table 1 Pearson's correlation coefficients between the density of OMP-positive cells in different layers of the olfactory epithelium and the amplitude of EOG responses

			Layer of the olfactory epithelium		
EOG responses		Total	Apical	Intermediate	Basal
Slow potentials	*r*	0.765	−0.388	−0.151	0.893
	(*P* value)	(0.118)	(0.694)	(0.576)	(0.054)
Oscillations	r	0.887	−0.315	−0.031	0.948[a]
	(*P* value)	(0.056)	(0.657)	(0.516)	(0.026)

[a]Statistically significant with $P < 0.05$, $n = 4$.

enhancement of EOG responses is explained by the increase in OMP-positive cells, especially those in the basal layer. For example, as to the amplitude of the EOGs evaluated by a negative slow potential (slow EOG), approximately 2-fold enhancement (0.45 vs. 0.99 mV) from the foraging period (October) to the breeding period (phase I) may be ascribed to 53% increase (580 vs. 890 cells/mm) in the OMP-positive cells in these periods. However, the enhancement of slow EOG may occur without the increase in the number of ORNs. Lidow et al. (1987) observed that the EOGs in frogs were progressively enhanced during regeneration of the ORNs after ablating the olfactory epithelium, but their physiological experiment did not show the increase in active ORNs. They suggested that the enhancement is rather due to morphological maturation of the ORNs: Matured ORNs have much longer cilia, and thus larger transduction area on the apical surface, resulting in the enhancement of the EOG responses. In the present study, the olfactory cilia were seen in the toads collected in both breeding and foraging periods, but quantitative data such as the length or number of the cilia to infer the maturation were not available. Instead, a progressive increase in the number of OMP-positive cells revealed in the present experiment implies the maturation of ORNs (Farbman and Margolis 1980; Margolis 1988). Therefore, the main contributors to the enhanced slow EOG in the breeding period would be the numerous, matured ORNs in the olfactory epithelium of the toads.

Significance of oscillatory potentials in the EOG

The enhancement of EOG responses in the early breeding period was more evident when the EOGs were evaluated by oscillations than by slow EOG. Increase in the OMP-positive cells is also more correlated with oscillations than with slow EOG. The density of OMP-positive cells in the basal layer, in particular, is highly correlated with oscillations. This may be ascribed to that oscillatory potentials superimposed on the EOGs more directly reflect the spiking activity of ORNs than slow EOG. In the salamander olfactory epithelium, application of the Na^+ channel blocker abolishes oscillatory potentials in the EOG without affecting slow EOG, suggesting that oscillations are attributed to synchronous spiking of the single neurons in the olfactory epithelium (Dorries and Kauer 2000). However, a recent study in channel catfish suggests that oscillatory potentials in the EOG do not necessarily originate from synchronous spiking but from a superposition of regular spike trains with similar interspike intervals (Díaz et al. 2007). In the toads of the early breeding period, the number of the OMP-positive cells was most elevated. The activity of many ORNs would generate an effective superposition, namely, a larger oscillation, if the activity of ORNs has properties that Díaz et al. (2007) showed in their simulation study (see Figure 6 in reference Díaz et al. 2007). To clarify the source of oscillations in the olfactory epithelium of the toads, the activity of single ORNs remains to be recorded.

An earlier study on the EOGs showed that oscillations in the olfactory epithelium were elicited only at very high odorant concentrations and only when the epithelium is mechanically injured (Ottoson 1956), namely in physiologically abnormal conditions, whereas recent studies show that they are elicited also at moderate concentrations (Dorries and Kauer 2000; Nikonov et al. 2002). In the olfactory epithelium of Japanese toads, oscillations were elicited by isoamyl acetate at concentrations of 0.5 mM or above. Therefore, oscillations are neuronal signals induced by the olfactory stimulation of normal physiological range. However, these concentrations were much higher than those to generate the slow EOG, suggesting that a larger population of receptor neurons activated by odorants is required to generate oscillations in the epithelium. Increase in the neurons in the epithelium would provide a higher chance of oscillations being generated. In a season when the toads track olfactory signals on a route to the breeding site, such an increase in the neurons was induced in the present study. Resultant enhancement of oscillations would provide a favorable condition for migrating toads to discriminate various odors in the environment because oscillatory potentials in the EOG are suggested to synchronize neural activities in the olfactory bulb, where processing of incoming

neural information takes place (Dorries and Kauer 2000; Nikonov et al. 2002).

Funding

Keio Gijuku Fukuzawa Memorial Fund for the Advancement of Education and Research (to T.N.) and Keio Gijuku Academic Development Funds (to H.N. and T.N.).

Acknowledgements

We are grateful to Dr Tadashi Nakamura (University of Electro-Communications) for his advice.

References

Abercrombie M. 1946. Estimation of nuclear population from microtome sections. Anat Rec. 94:239–247.

Adrian ED. 1955. Potential oscillations in the olfactory organ. J Physiol (Lond). 128(Suppl):21P–22P.

Adrian ED. 1956. The action of the mammalian olfactory organ. J Laryngol Otol. 70:1–14.

Berven KA, Grudzien TA. 1990. Dispersal in the wood frog (*Rana sylvatica*): implications for genetic population structure. Evolution. 44:2047–2056.

Dawley EM. 1998. Olfaction. In: Heatwole H, Dawley EM, editors. Amphibian biology, volume 3, sensory perception. Chipping Norton (UK): Surrey Beatty and Sons. p. 711–742.

Dawley EM, Crowder J. 1995. Sexual and seasonal differences in the vomeronasal epithelium of the red-backed salamander (*Plethodon cinereus*). J Comp Neurol. 359:382–390.

Dawley EM, Fingerlin A, Hwang D, John SS, Stankiewicz CA. 2000. Seasonal cell proliferation in the chemosensory epithelium and brain of red-backed salamanders, *Plethodon cinereus*. Brain Behav Evol. 56: 1–13.

Díaz J, Razeto-Barry P, Letelier J-C, Caprio J, Bacigalupo J. 2007. Amplitude modulation patterns of local field potentials reveal asynchronous neuronal populations. J Neurosci. 27:9238–9245.

Dingle H. 1996. Migration: the biology of life on the move. New York: Oxford University Press.

Dole JW. 1968. Homing in leopard frogs, *Rana pipiens*. Ecology. 49: 386–399.

Dorries KM, Kauer JS. 2000. Relationships between odor-elicited oscillations in the salamander olfactory epithelium and olfactory bulb. J Neurophysiol. 83:754–765.

Farbman AI. 1990. Olfactory neurogenesis: genetic or environmental control? Trends Neurosci. 13:362–365.

Farbman AI, Margolis FL. 1980. Olfactory marker protein during ontogeny: immunohistochemical localization. Dev Biol. 74:205–215.

Ferrando S, Bottaro M, Gallus L, Girosi L, Vacchi M, Tagliafierro G. 2007. First detection of olfactory marker protein (OMP) immunoreactivity in the olfactory epithelium of a cartilaginous fish. Neurosci Lett. 413: 173–176.

Ghose GM, Freeman RD. 1992. Oscillatory discharge in the visual system: does it have a functional role? J Neurophysiol. 68:1558–1574.

Gill DE. 1978. Effective population size and interdemic migration rates in a metapopulation of the red-spotted newt, *Notophthalmus viridescens* (Rafinesque). Evolution. 32:839–849.

Graves BM. 1994. The role of nasolabial grooves and the vomeronasal system in recognition of home area by red-backed salamanders. Anim Behav. 47:1216–1219.

Gray CM, Singer W. 1989. Stimulus-specific neuronal oscillations in orientation columns of cat visual cortex. Proc Natl Acad Sci USA. 86:1698–1702.

Graziadei PPC, Monti-Graziadei GA. 1978. Continuous nerve cell renewal in the olfactory system. In: Jacobson M, editor. Handbook of sensory physiology IX, development of sensory systems. Berlin (Germany): Springer-Verlag. p. 55–83.

Grubb JC. 1973. Olfactory orientation in *Bufo woodhousei fowleri, Pseudacris clarki* and *Pseudacris streckeri*. Anim Behav. 21: 726–732.

Ishii S, Kubokawa K, Kikuchi M, Nishio H. 1995. Orientation of the toad, *Bufo japonicus*, toward the breeding pond. Zool Sci. 12: 475–484.

Keller A, Margolis FL. 1975. Immunological studies of the rat olfactory marker protein. J Neurochem. 24:1101–1106.

Kiviranta H, Tuomainen A, Reiman M, Laitinen S, Liesivuori J, Nevalainen A. 1998. Qualitative identification of volatile metabolites from two fungi and three bacteria species cultivated on two media. Cent Eur J Public Health. 6:296–299.

Krishna NS, Getchell TV, Margolis FL, Getchell ML. 1992. Amphibian olfactory receptor neurons express olfactory marker protein. Brain Res. 593:295–298.

Kusano T, Maruyama K, Kaneko S. 1995. Post-breeding dispersal of the Japanese toad, *Bufo japonicus formosus*. J Herpetol. 29: 633–638.

Kusano T, Maruyama K, Kaneko S. 1999. Breeding site fidelity in the Japanese toad, *Bufo japonicus formosus*. Herpetol J. 9:9–13.

Lam Y-W, Cohen LB, Wachowiak M, Zochowski MR. 2000. Odors elicit three different oscillations in the turtle olfactory bulb. J Neurosci. 20: 749–762.

Lema SC, Nevitt GA. 2004. Evidence that thyroid hormone induces olfactory cellular proliferation in salmon during a sensitive period for imprinting. J Exp Biol. 207:3317–3327.

Lidow MS, Gesteland RC, Shipley MT, Kleene SJ. 1987. Comparative study of immature and mature olfactory receptor cells in adult frogs. Brain Res. 428:243–258.

Lledo PM, Alonso M, Grubb MS. 2006. Adult neurogenesis and functional plasticity in neuronal circuits. Nat Rev Neurosci. 7:179–193.

Margolis FL. 1972. A brain protein unique to the olfactory bulb. Proc Natl Acad Sci USA. 69:1221–1224.

Margolis FL. 1988. Molecular cloning of olfactory specific gene products. In: Margolis FL, Getchell TV, editors. Molecular neurobiology of the olfactory system. New York: Plenum Press. p. 237–265.

Monti-Graziadei GA, Margolis FL, Harding JW, Graziadei PPC. 1977. Immunocytochemistry of the olfactory marker protein. J Histochem Cytochem. 25:1311–1316.

Moriya-Ito K, Osada T, Ishimatsu Y, Muramoto K, Kobayashi T, Ichikawa M. 2005. Maturation of vomeronasal receptor neurons in vitro by coculture with accessory olfactory bulb neurons. Chem Senses. 30: 111–119.

Moulton DG. 1974. Dynamics of cell populations in the olfactory epithelium. Ann N Y Acad Sci. 237:52–61.

Nakazawa H, Kaji S, Ishii S. 2000. Oscillatory electric potential on the olfactory epithelium observed during the breeding migration period in the Japanese toad, *Bufo japonicus*. Zool Sci. 17:293–300.

Nikonov AA, Parker JM, Caprio J. 2002. Odorant-induced olfactory receptor neural oscillations and their modulation of olfactory bulbar responses in the channel catfish. J Neurosci. 22:2352–2362.

Ottoson D. 1956. Analysis of the electrical activity of the olfactory epithelium. Acta Physiol Scand. 35(Suppl 122):1–83.

Ottoson D. 1958. The slow electrical response of the olfactory end organs. Exp Cell Res Suppl. 5:451–459.

Phillips JB. 1987. Laboratory studies of homing orientation in the Eastern red-spotted newt (*Notophthalmus viridescens*). J Exp Biol. 131: 215–229.

Pilliod DS, Peterson CR, Ritson PI. 2002. Seasonal migration of Columbia spotted frogs (*Rana luteiventris*) among complementary resources in a high mountain basin. Can J Zool. 80:1849–1862.

Riddle DR, Oakley B. 1992. Immunocytochemical identification of primary olfactory afferents in rainbow trout. J Comp Neurol. 324: 575–589.

Schmidt RS. 1984. Mating call phonotaxis in the female American toad: induction by hormones. Gen Comp Endocrinol. 55:150–156.

Schomburg D, Schomburg I, Chang A. 2006. Alcohol O-acetyltransferase. In: Schomburg D, Schomburg I, Chang A, editors. Springer handbook of enzymes vol. 30, class 2 transferases III. Berlin (Germany): Springer-Verlag. p. 125–130.

Shibuya T, Tucker D. 1967. Single unit responses of olfactory receptors in vultures. In: Hayashi T, editor. Olfaction and taste II. New York: Pergamon Press. p. 219–233.

Sinsch U. 1987. Orientation behaviour of toads (*Bufo bufo*) displaced from the breeding site. J Comp Physiol A. 161:715–727.

Sinsch U. 1992. Sex-biased site fidelity and orientation behavior in reproductive natterjack toads (*Bufo calamita*). Ethol Ecol Evol. 4:15–32.

Stille WT. 1952. The nocturnal amphibian fauna of the southern Lake Michigan beach. Ecology. 33:149–162.

Stopfer M, Bhagavan S, Smith BH, Laurent G. 1997. Impaired odour discrimination on desynchronization of odour-encoding neural assemblies. Nature. 390:70–74.

Sutterlin AM, Sutterlin N. 1971. Electrical responses of the olfactory epithelium of Atlantic salmon (*Salmo salar*). J Fish Res Board Can. 28:565–572.

Suzuki N, Takahata M, Shoji T, Suzuki Y. 2004. Characterization of electro-olfactogram oscillations and their computational reconstruction. Chem Senses. 29:411–424.

Takagi SF, Shibuya T. 1960. Potential oscillations in the lower olfactory pathway of the toad. Nature. 186:724.

Takagi SF, Yajima T. 1964. Electrical responses to odours of degenerating olfactory epithelium. Nature. 202:1220.

Takigami S, Wakabayashi Y, Ohsako S, Ohkura S, Okamura H, Ikai A, Ichikawa M, Osada T. 2004. Fetal development of vomeronasal system in the goat. Brain Res Dev Brain Res. 149:113–120.

Tucker D. 1975. Waves elicited from peripheral neural tissue (olfactory) in response to odorous stimulation. Biophys J. 15:271a.

Twitty VC. 1959. Migration and speciation in newts. Science. 130:1735–1743.

Verhaagen J, Oestreicher AB, Gispen WH, Margolis FL. 1989. The expression of the growth associated protein B50/GAP43 in the olfactory system of neonatal and adult rats. J Neurosci. 9:683–691.

Whitford WG, Vinegar A. 1966. Homing, speed of migration, over-wintering of larvae, and sex-ratio in breeding populations of *Ambystoma maculatum*. Copeia. 1966:515–519.

Accepted July 8, 2009